

# Analysis and Design of a DC/DC ZVS PWM Off-Line Converter

J. R. Pinheiro, T. F. Pegoraro and J. E. Baggio

Federal University of Santa Maria

CT/DEL/NUPEDEE

97.119-900 - Santa Maria - RS - BRAZIL

**Abstract:** A complete analysis and characterization of a DC/DC ZVS PWM off-line converter are presented. The regions of soft-switching for all the semiconductor devices are identified. The dc/dc converter is composed by a half-bridge on the input side and a double-boost on the output side. The analyzed DC/DC converter presents low switching losses (ZVS), low device and component stresses, simple control, step-up/down operation (boost-buck), and it operates ZVS at a wide load range. Therefore, the combination of these attributes results in a high power density and efficient converter.

Principle of operation, theoretical analysis, design procedure and an example along with laboratory experimental results are presented to demonstrate the feasibility and validation of the theoretical analysis.

## I. INTRODUCTION

DC/DC ZVS PWM converters have some advantages such as low devices and components stresses, it permits to incorporate a large number of the parasitic elements, high efficiency and PWM control at constant switching frequency when it is compared with the resonant converters counterparts.

The ZVS full-bridge phase-shifted converters [7,8,9] are suitable for high power applications. For operation in a wide range of load are necessary auxiliary commutation circuits, which in general form increases, the circulating reactive energy, resulting in an increase of the conduction losses. If a ZVS half-bridge converter is chosen, it is classical to regulate it by FM (frequency modulation) to control the output power transference, since the duty-cycle is equal to 50% to achieve ZVS. On the other hand, if this converter operates at constant frequency it is necessary a power control element such as a linear variable inductor [5] or even including another converter.

An attractive approach for high power is the phase-shifted dual active bridge DC/DC converter [1,2]. This converter have the most favorable characteristics: low device and component stresses, ZVS for all devices, small filter components, high efficiency (no trapped energy), bi-directional power flow, buck-boost operation possibility, low sensitivity to system parasitic components and due to its characteristic of current transfer makes it appropriated for applications where parallel multiple modules are necessary to extend the power capacity of the system. A disadvantage of this converter is that the output capacitive DC filter must

carry high ripple current. Therefore, this converter is not suitable for the high output current applications which also require low output voltage ripple. On the other hand, it is very robust, due to its natural ability to sustain an overload or even an output short-circuit. It presents a current source output characteristic appropriated for some applications, such as: battery chargers, welding, aerospace sources, distributed power sources and parallel multiple module systems.

This paper presents an isolated ZVS-PWM DC/DC converter, which presents some characteristics similar to presented in [1,2], but differ essentially in the following parts: smaller number of components, unidirectional power flow, PWM control and it may operate at ZVS independently of the load value as step-up as step-down mode.

## II. DC/DC ZVS PWM CONVERTER DESCRIPTION

The analyzed topology in this paper is shown in Fig.1. It consists of two stages: one stage of voltage inversion and another of active rectification and filtering. In the primary side is utilized a half-bridge converter formed by two controlled switches ( $S_1, S_2$ ), two diodes ( $D_{S1}, D_{S2}$ ), two symmetric DC sources ( $E_1, E_2$ ) that may be a DC source with a capacitive sharing. High-frequency transformer ( $T$ ) makes the linking and galvanic isolation between the two stages. In the secondary side, it includes an inductor ( $L$ ) of energy transfer between the input and the output, four rectifiers diodes at full bridge topology ( $D_3, D_4, D_5, D_6$ ), two switches ( $S_3, S_4$ ) forming a double-boost permitting perform the power flow control, capacitive output filter ( $C_f$ ) and the load ( $R_L$ ). Here it is important to point out that the resonant inductor can be placed as in the primary side as in the secondary one.

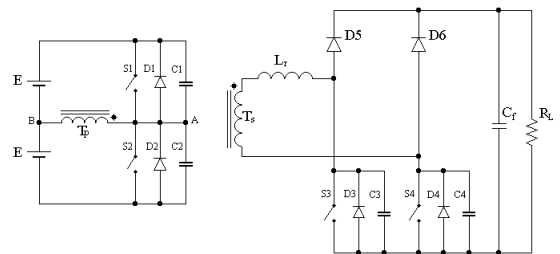


Fig. 1. DC/DC ZVS PWM Off-line Converter

The DC/DC ZVS PWM off-line converter presents three operation modes. Depending of the duty cycle and of the load, different operation modes of the circuit can occur. Each

one of these presents a unique device conduction sequence, resulting in different output behaviors.

### III. DESCRIPTION OF THE OPERATION STAGES

To describe the operation of the DC/DC ZVS PWM off-line converter, it is assumed that all the components are ideals, the output is represented by a constant voltage source and the circuit is working in steady-state.

The operation stages of each operation mode are described as follow:

#### A. Continuous Conduction Mode I - CCM I

1) *First Stage* ( $\Delta T_1$ ): This stage begins at instant in which  $S_2$  is turned off and  $S_1$  is gated on. The inductor current flows through the capacitors  $C_1$  and  $C_2$ , increasing the  $S_2$  voltage up to  $2E$  and decreasing the voltage on  $S_1$  to zero. The switches  $S_3$  and  $S_4$  are enable to conduct, however only  $S_4$  is gated on. Inductor current is negative, however its temporal derived is positive. There is transfer power from the inductor to both load and input source.  $V_L = E + V_o$ . (Fig. 2.a)

2) *Second Stage* ( $\Delta T_2$ ): When the inductor current reaches zero, it begins the boost stage. Now, the diode  $D_3$  conducts, then the  $S_3$  switch is able to turn on. In this stage, there is not power transference to load. The inductor current  $i_L$  increases linearly, because  $V_L = E$ . (Fig. 2.b)

3) *Third Stage* ( $\Delta T_3$ ): The two boost switches  $S_3$  and  $S_4$  are turned off and the diode  $D_6$  is directly polarized. As the output voltage is higher than the input voltage, the inductor current  $i_L$  begins to decrease linearly. The input source and the inductor transfer energy to the load.  $V_L = E - V_o$ . (Fig. 2.c)

4) *Fourth Stage* ( $\Delta T_1$ ): It begins when the switches  $S_1$  and  $S_2$  commutate at ZVS and  $S_3$  is turned on because its anti-parallel diode  $D_3$  conducts current  $i_L$ . In the same form as occurs in the first stage, there is power transfer from the inductor to the load and to the input source.  $V_L = -(E + V_o)$ . (Fig. 2.d)

5) *Fifth Stage* ( $\Delta T_2$ ): Such as in the second stage, when the inductor current reaches zero, it begins the boost stage. Now, the diode  $D_4$  conducts, then the  $S_4$  switch is able to turn on. In this stage, there is not power transfer to load. The inductor current  $i_L$  decreases linearly, because  $V_L = -E$ . (Fig. 2.e)

6) *Sixth Stage* ( $\Delta T_3$ ): The two boost switches  $S_3$  and  $S_4$  are turned off and the diode  $D_5$  is directly polarized. As the output voltage is higher than the input voltage, the inductor current  $i_L$  begins to increase in a linear fashion. The input source and the inductor transfer energy to the load.  $V_L = -E + V_o$ . (Fig. 2.f)

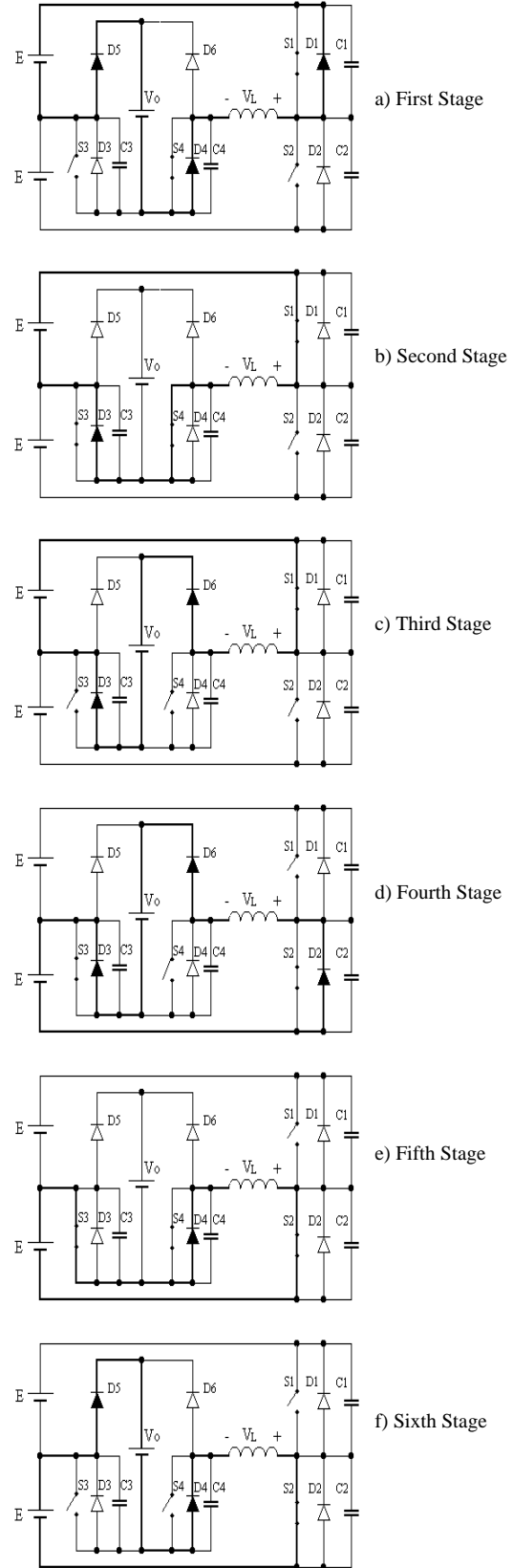


Fig.2. Operation Stages for the CCM I.

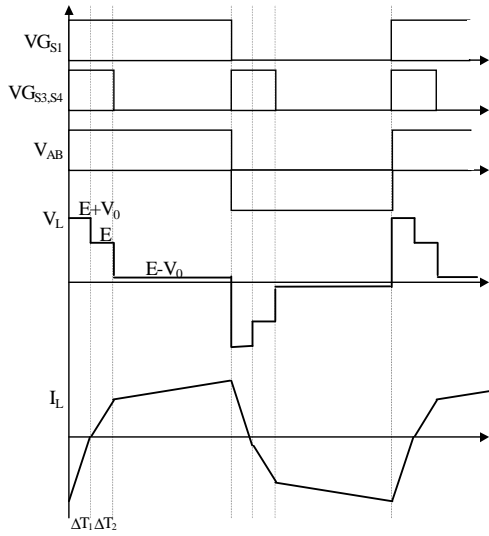


Fig.3. CCM I Waveforms.

### B. Continuous Conduction Mode II - CCM II

This mode is similar to CCM I. The main difference is that the converter at the CCM I can operate like a step-up (boost) or step-down (buck) and at the CCM II it operates only like a step-down (buck), moreover in this mode is not possible to regulate the output voltage. Therefore the sequences of operation are such as to that of the CCM I, differing only by the absent of the second and fourth stages. In this mode, the output converter operates as a passive rectifier.

### C. Discontinuous Conduction Mode - DCM

1) *First Stage:* This is a boost stage, the inductor current  $i_L$  flows through  $S_1$ ,  $L$ ,  $S_4$ ,  $S_3/D_3$  and upper input source. Therefore, inductor current  $i_L$  increases in a linear fashion. Input source energy is transfer to inductor, however none is transferred to output filter.  $V_L=E$ . (Fig. 4.a)

2) *Second Stage:* The two boost switches  $S_3$  and  $S_4$  are turned off and the  $D_6$  is directly polarized. The inductor current  $i_L$  begins to decrease linearly because the output voltage is higher than input voltage. The input source and the inductor transfer energy to load.  $V_L=E-V_o$ . (Fig. 4.b)

3) *Third Stage:* It begins at instant that the inductor current reaches zero. During all this stage the inductor current stays null, and the output diodes do not conduct because  $V_o \geq E$ .  $V_L=0$ . (Fig.4.c)

4) *Fourth Stage:*  $S_1$  is turned off and the switch  $S_2$  is gated on. This commutation can be at ZVS mode, if the magnetizing inductance of the HF transformer is designed adequate or even if an auxiliary commutation inductor is included in the circuit. Alike than it was discussed in the CCM I and II, here the switches  $S_3$  and  $S_4$  are commuted on hard form (dissipative) and the inductor current decreases linearly.  $V_L=-E$ . (Fig. 4.d)

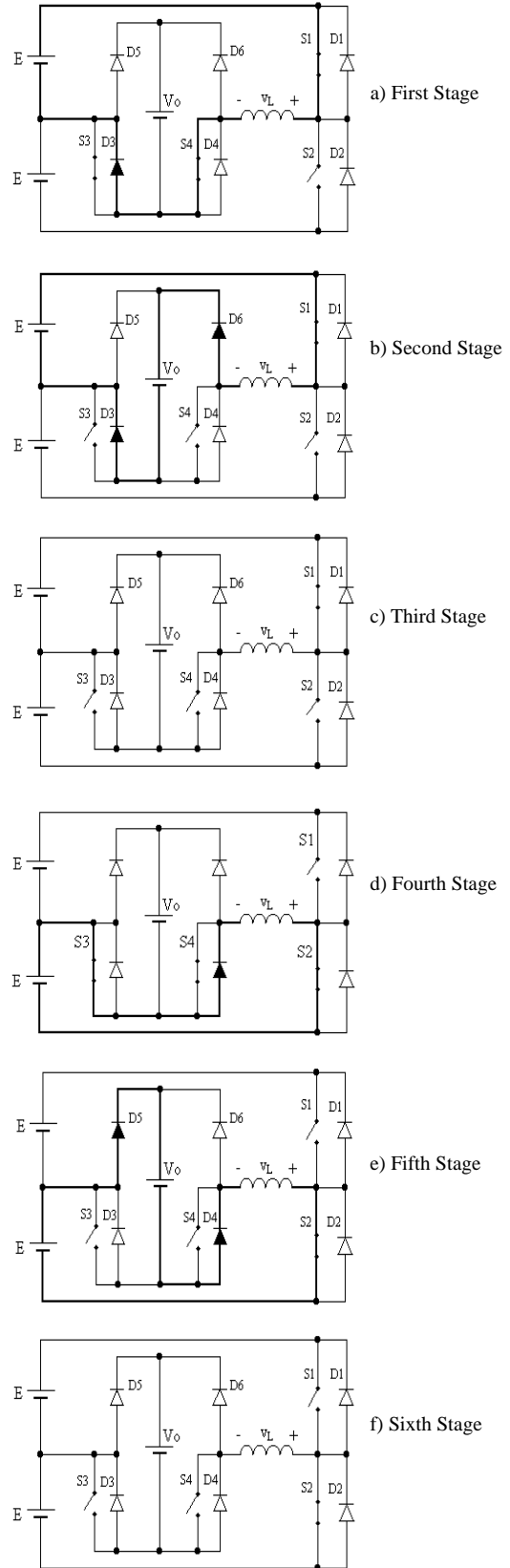


Fig.4. Operation Stages for the DCM.

5) *Fifth Stage*: The switches of the secondary side are turned off. The inductor stored energy is transferred to the load. It finishes at the moment in which the inductor current becomes null.  $V_L = -(E + V_o)$ . (Fig. 4.e)

6) *Sixth Stage*: The same form as it occurred in the third stage, there is not current flowing by inductor even that  $S_2$  were closed, because the output voltage  $V_o$  is higher than the input one.  $V_L = 0$ . (Fig. 4.f)

#### IV. ANALYSIS OF THE CONVERTER

To analyze completely the converter, firstly it is necessary to identify all possible circuit operation modes, in which each one represents a unique conduction sequence of switching devices. Therefore, resulting in different waveforms and commutation requirements. The time interval  $\Delta T_2$  is assigned as the effective duty cycle.

##### A. Continuous Conduction Mode - CCM I

To obtain the characteristic equation it is imperious to have a priori the knowledge of every operation sequence, each one represented by a differential equation. Therefore, from the equations referent to intervals  $\Delta T_1$ ,  $\Delta T_2$ , and  $\Delta T_3$  corresponding to a semi-period, it can derive the output voltage equation, as well as all equations of interest.

The output voltage is given by:

$$n.V_o = \frac{9.x^2 - 3.b + a^2}{9.x} \quad (1)$$

where:

$$a = \frac{E}{f.L} \cdot [R.(1-D)^2 + 4.f.L]$$

$$b = \frac{E^2}{2.f.L} \cdot [R.(4.D^2 - 4.D - 1) + 8.f.L]$$

$$c = \frac{R.E^3}{2.f.L} \cdot (4.D^2 - 4.D - 1)$$

$$x = \sqrt[3]{\frac{a.b}{6} - \frac{a^3}{27} - \frac{c}{2} + \frac{\sqrt{3}}{18} \cdot \sqrt{4.a^3.c - a^2.b^2 - 18.a.b.c + 4.b^3 + 27.c^2}}$$

being  $n$  the transformer turns ratio

##### B. Continuous Conduction Mode - CCM I

In this mode,  $\Delta T_2 = 0$  and the output voltage can not be controlled by the active switches. The variables are given by:

$$\Delta T_1 = \frac{R + 2.f.L - \sqrt{4.f^2.L^2 + R^2}}{2.f.R} \quad (2)$$

$$nV_o = -\frac{E}{R} \cdot (2.f.L - \sqrt{4.f^2.L^2 + R^2}) \quad (3)$$

##### C. Discontinuous Conduction Mode - DCM

For a resistive load, the following equation was found:

$$n.V_o = E + E.R \cdot \frac{D^2}{f.L \left( 1 + \sqrt{1 + 2.R \cdot \frac{D^2}{f.L}} \right)} \quad (4)$$

The system works as a step-up converter, such as a boost converter operating at discontinuous mode. Extra auxiliary circuits are necessary to perform soft commutation.

The boundaries between CCM and DCM known as critical condition is given by the equation below:

$$nV_o = \frac{E}{1 - D_{c1}} \quad (5)$$

The boundary between the CCM I and CCM II is determined by:

$$nV_o = E \cdot (1 - 2.D_{c2}) \quad (6)$$

#### V. DESIGN METHODOLOGY:

Initially, some specifications are defined to project the converter, they are:

$P_{out} = 250W$	(Output Power)
$2E = 270V$	(Input Voltage)
$V_o = 90V$	(Output Voltage)
$f = 200kHz$	(Switching Frequency)

From the analytical study of the losses equation of the converter, it has been obtained for a duty cycle equal to 0.3 the maximum efficiency.

To operate only in the CCM I, controlling the output voltage for a duty cycle range from 0 to 1, the output voltage gain must be unitary, as can be seen in Fig 10. The transformer turns ratio is:

$$n = \frac{E}{g.V_o} = 1,5 \quad (7)$$

where  $g$  is the output voltage gain

Choosing the duty cycle and the output voltage gain, the inductor value is obtained as follows:

$$L_r = \frac{E.R}{2.f.nV_o} \cdot \left\{ \frac{-2.D^2 \cdot [(E + nV_o)^2]}{4.E^2 + 4.EnV_o + n^2V_o^2} + \frac{4.D \cdot [(E + nV_o)^2 - E.nV_o] + (E^2 + E.nV_o - 2.nV_o^2)}{4.E^2 + 4.E.nV_o + n^2V_o^2} \right\} \quad (8)$$

$$L_r = 41\mu H$$

#### VI. EXPERIMENTAL RESULTS

Based on the design methodology discussed in the previous item, a prototype was implemented and tested in the laboratory. By the comparison between the theoretical,

simulations and their respective experimental waveforms and curves, it can be observed that these data are very close. Therefore, operation principle of the analyzed converter is validated.

Table I presents the components values and power semiconductor devices utilized in the breadboard, along with their manufactory code names.

In Fig.5 are shown the drain-source voltage of the main power switch of the inverter (primary converter) and its gate-source voltage. It can be seen the ZVS command action. The gate-source voltage is applied only after the drain-source voltage reaches zero. The power switches of the double-boost (secondary converter) also operate at the ZVS mode; it can be seen by Fig. 6.

As the converter is operating in the CCM I, it can operate in three different modes, namely: step-up, set-down and unitary voltage gain. These modes are depicted in the figures 7, 8 and 9, respectively.

External characteristic curves of the DC/DC ZVS PWM off-line converter, i.e., the output/input voltage ratio in function of the duty-cycle for a constant load ( $R = 25\Omega$ ) obtained experimentally is shown by Fig. 10.

TABLE I  
COMPONENTS AND DEVICES UTILIZED IN THE PROTOTYPE

Component	Parameter
S1, S2, S3, S4	MOSFET IRF740
D1, D2, D3, D4	MOSFET intrinsic diode
C1, C2, C3, C4	MOSFET intrinsic capacitor
D5, D6	HFA08PB60
$C_f$	1mF/550V
HF transformer	EE 55/21- 9 primary turns and 6 secondary turns (3:2) - Thornton
Inductor	41 $\mu$ H - EE 42/15 - 18 turns - Thornton

The design targeted the maximization of the efficiency of the converter, that for this particular case occurs at duty-cycle equal to 0.3. It is illustrated by Fig. 11, in which a maximum efficiency (90%) is obtained at the rated load ( $D=0.3 @ 250W$ ).



Fig. 5: 1> S1 Drain-Source Voltage (50V/div);  
2> S1 Gate-Source Voltage (10V/div) - 1 $\mu$ s/div.

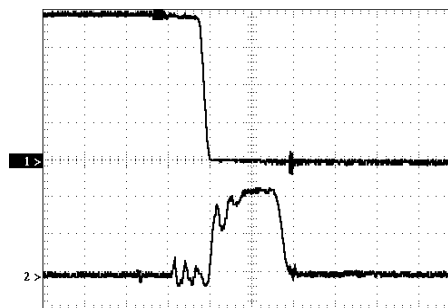


Fig. 6: 1> S3 Drain-Source Voltage (50V/div);  
2> S3 Gate-Source Voltage (5V/div) - 500ns/div.

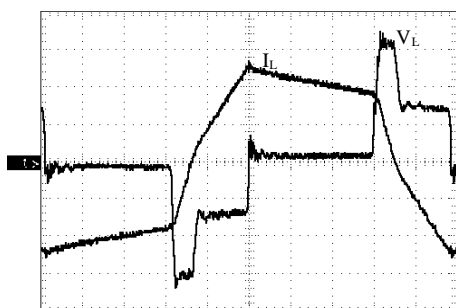


Fig. 7: Inductor Current (1A/div) and Voltage (50V/div)  
for  $g > 1$  - 1 $\mu$ s/div

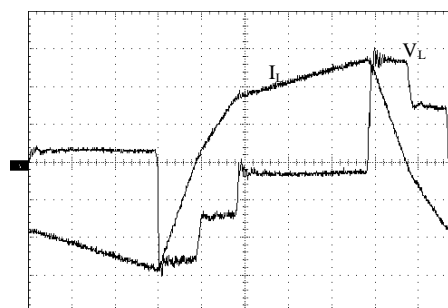


Fig. 8: Inductor Current (1A/div) and Voltage (50V/div)  
for  $g < 1$  - 1 $\mu$ s/div

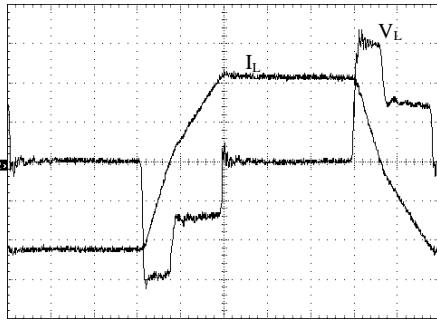


Fig. 9: Inductor Current (1A/div) and Voltage (50V/div) for  $g = 1 - 1\mu\text{s/div}$

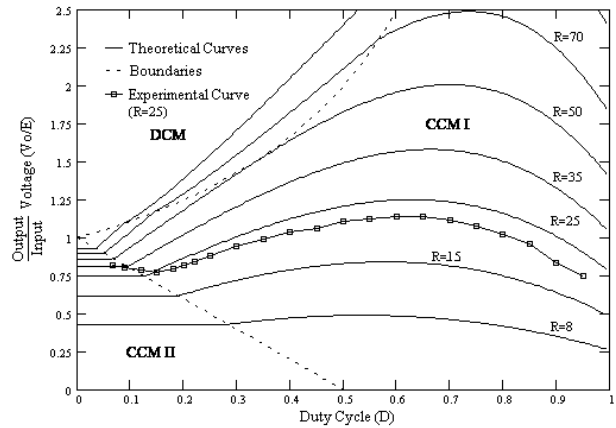


Fig.10 - Characteristic curves.

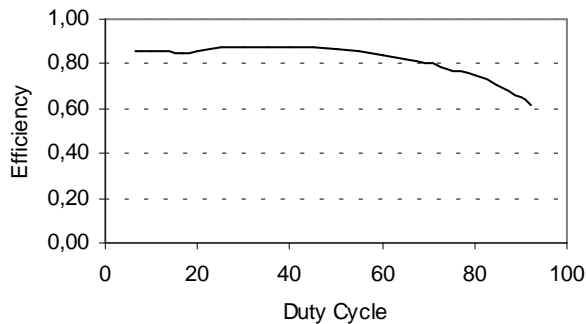


Fig. 11 - Efficiency x Duty Cycle curve

## VI. CONCLUSIONS

In this paper has been studied, analyzed and implemented a DC/DC ZVS PWM off-line converter. It is identified and described all operation stages. By the mathematical analysis is possible to determine the characteristic curves and main equations of the converter, which permits designers to project the converter parameters and the components values.

The DC/DC ZVS PWM off-line converter is formed by a half-bridge converter on primary side and a double-boost on secondary one. From the experimental results, it can mention that it presented low switching losses, simple control (PWM), step-up/down operation and ZVS operation for a wide load range. The combination of the above mentioned attributes results in a high power density and efficient converter. Moreover, it is very robust due to its natural ability to sustain overload and even output short-circuits.

It presents an attractive current source output characteristic appropriated for some applications, such as: battery chargers, welding, aerospace sources, distributed power sources and parallel multiple module systems.

## REFERENCES

- [1] - R.W.A.A De Doncker, D.M. Divan, MH. Kheraluwala - "A Three-Phase Soft-Switched High-Power-Density dc/dc Converter for High-Power Applications" - Proceeding of the IEEE Industry Applications Society Annual Meeting, Oct.1988, pp.796-805.
- [2] - M.H. Kheraluwala, R.W. Gascoigne, D.M. Divan, E. Bauman - "Performance Characterization of a High Power Dual Active Bridge dc/dc Converter" - Proceeding of the IEEE Industry Applications Society Annual Meeting, 1990, pp.1267-1273.
- [3] - D. Patterson, D. M. Divan - "Pseudo-Resonant Full Bridge dc/dc Converter" - IEEE PESC Record, 1987, pp.424-430.
- [4] - A.J. Perin, I. Barbi - "A New Isolated Half-Bridge Soft-Switching Pulse-Width Modulated DC-DC Converter" - Record of IEEE APEC, Feb.1992, pp.66-72.
- [5] - A.S. Kilowski - "Half-Bridge Power-Processing Cell Utilizing a Linear Variable Inductor and Thyristor-Dual Switches" - IEEE PESC Record, 1988, pp.284-289.
- [6] - K. Harada, Y. Ishihara and Todaka - "Analysis and Design of ZVS-PWM Half-Bridge Converter with Secondary Switches" - IEEE PESC Record, 1995, pp.280-284.
- [7] - J. A. Sabate and F.C. Lee - "Off-Line Application of the Fixed Frequency Clamped Mode Series-Resonant Converter" - APEC'89 Proceedings, pp.213-220.
- [8] - R. Fischer, K.D.T. Ngo, M.H.Kuo - "A 500KHz, 250W DC-to-DC Converter with Multiple output Controlled by Phase-Shift PWM and Magnetic Amplifiers" High Frequency power Conversion Conf., 1998, pp.100-110.
- [9] - J. A. Sabate, V. Vlatkovic, R.B. Ridley, F.C. Lee and B.H. Cho - "Design Considerations for high Power Full-Bridge ZVS PWM Converter" - IEEE APEC conf. Proceedings, 1990, pp.275-284.